Investigating the impact of atmospheric conditions on wake-steering performance at a commercial wind plant

Eric Simley, Mithu Debnath and Paul Fleming

National Wind Technology Center, National Renewable Energy Laboratory, Golden, CO, 80401, USA

E-mail: eric.simley@nrel.gov
Keywords: Wind farm control, wake steering, atmospheric stability, turbulence

Abstract. Wake steering is a wind farm control strategy in which upstream wind turbines are misaligned with the wind to deflect their wakes away from downstream turbines, thereby increasing net energy production. But research suggests that the effectiveness of wake steering strongly depends on atmospheric conditions such as stability. In this paper, we investigate results from a two-turbine wake-steering experiment at a commercial wind plant to assess the impact of stability and five other atmospheric variables on wake-steering performance. Specifically, for different atmospheric condition bins we compare the ability of the controller to achieve the intended yaw offsets, the power gain from wake steering, and the reduction in wake losses. Further, we analyze wake-steering performance as a function of wind speed to eliminate the confounding impact of different wind speed distributions in different atmospheric conditions. Overall, we find that wind direction standard deviation is the best predictor of wake-steering performance, followed by turbulence intensity and turbulent kinetic energy. The results suggest the importance of adapting wake-steering control strategies to different atmospheric conditions.

1. Introduction

Wake steering is a wind farm control strategy for increasing energy production and reducing structural loads in which upstream wind turbines are misaligned with the wind to deflect their wakes away from downstream turbines [1]. In addition to promising results using high-fidelity modeling [2], several recent field experiments at commercial wind plants have demonstrated significant energy gains from wake steering [3]–[7].

Notwithstanding the overall potential for wake steering, research suggests that the effectiveness of the control strategy strongly depends on atmospheric conditions. Using large-eddy simulation, Vollmer *et al.* [8] find that the ability to deflect a wind turbine's wake increases for stable atmospheric boundary layers (ABLs), with little benefit expected during more turbulent, unstable ABLs. Through a wake-steering experiment at a commercial wind plant, Fleming *et al.* [4, 5] measure larger energy improvements in stable ABLs [4] and during the nighttime, when the atmosphere is typically more stable [5]. For the same field campaign, Hamilton [9] shows that energy gains from wake steering are greater during more stationary conditions, accounting for variations in wind direction, wind speed, and turbulence intensity. Additionally, analyses of operational wind plants reveal how wake losses are significantly higher

in stable ABLs, with lower turbulence intensity, at commercial offshore [10] and land-based [11] wind plants; these conditions are expected to provide more opportunity for wake steering to *reduce* wake losses. Lastly, using the National Renewable Energy Laboratory's computationally efficient FLOw Redirection and Induction in Steady State (FLORIS) engineering wind farm control tool [12] to estimate the energy gain from wake steering for a set of 60 existing U.S. wind plants, Bensason *et al.* [13] estimate that the average improvement in annual energy production increases from 0.6% to 1.1% for fixed turbulence intensities of 10% and 6%, respectively.

In this paper, we extend the analysis of the wake-steering field experiment presented by Fleming *et al.* [4, 5] to assess the influence of stability, turbulence intensity, and four other atmospheric variables on the effectiveness of wake steering. However, whereas Fleming *et al.* combined measurements for a wide range of wind speeds when comparing wake steering in stable and unstable ABLs [4] as well as during the daytime and nighttime [5], we analyze performance as a function of wind speed; this helps eliminate the confounding impact of distinct wind speed distributions during different atmospheric conditions because the effectiveness of wake steering naturally varies with wind speed through changes in the wind turbines' power and thrust coefficients. Specifically, for a given wind speed range, we divide the measurement data into two bins based on the atmospheric variable of interest. We then compare three performance metrics using data from the two bins: the error between the measured and intended yaw offsets as well as the relative change in power and reduction in wake losses with wake steering.

The rest of the paper is organized as follows. We provide an overview of the wake-steering field experiment in Section 2, followed by a discussion of the atmospheric variables investigated in Section 3. Next, the analysis methods are described in Section 4. The impact of the different atmospheric conditions on wake-steering performance is then presented in Section 5. Lastly, Section 6 concludes the paper with a discussion of the results and suggestions for further research.

2. Field experiment overview

In this section, we present a brief overview of the wake steering experiment, conducted using a subset of wind turbines at a commercial wind plant in the U.S. between May 2018 and February 2020. A more thorough discussion of the experiment is provided by Fleming *et al.* [4, 5].

2.1. Experiment configuration

The layout of the wake-steering experiment is shown in Figure 1. All five wind turbines have a rated power of 1.5 MW, rotor diameter (D) of 77 m, hub height of 80 m, and rated wind speed of ∼14 m/s. Turbines T2 and T4 were controlled to deflect their wakes away from turbine T3, whereas turbines T1 and T5 acted as freestream references. Turbines T2 and T4 were toggled hourly between baseline and wake-steering control, allowing the two control modes to be compared during similar atmospheric conditions. The campaign was divided into a south experiment—which focused on wake interactions between turbines T4 and T3—and a north experiment, in which turbine T2 was controlled to benefit turbine T3, $5D$ downstream, between January 2019 and February 2020 [4, 5]. A 60-m meteorological (met) tower and a WindCube v2 profiling lidar were located northwest of turbine T2.

In this paper, we concentrate on the north experiment, in which yaw offsets are applied to turbine T2 for wind directions between 324° and 347° to take advantage of the freestream wind measurements provided by the met tower as well as the simple terrain upstream of the wind turbines. Because the met tower does not reach the turbine hub height, and lidar measurements were frequently unavailable during the experiment, the inflow wind speed and wind direction are estimated using the average wind speed measured by the nacelle anemometers on reference turbines T1 and T5 and the average nacelle orientation of the two reference turbines, respectively. Distributions of the wind speeds and wind directions analyzed in this paper are shown in Figure 2.

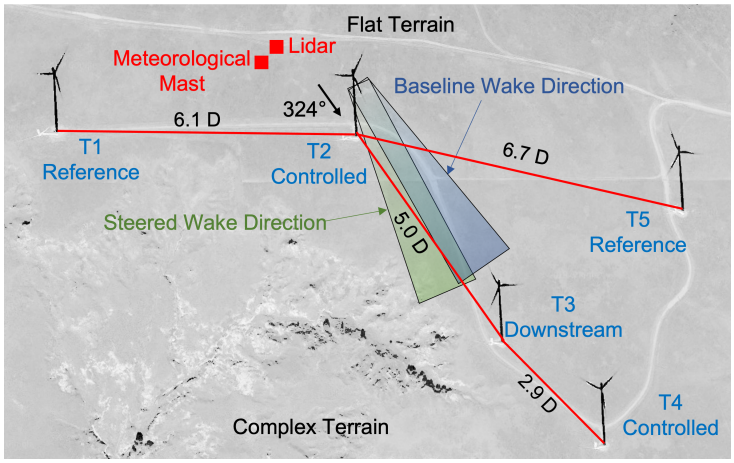

Figure 1. Wind plant layout.

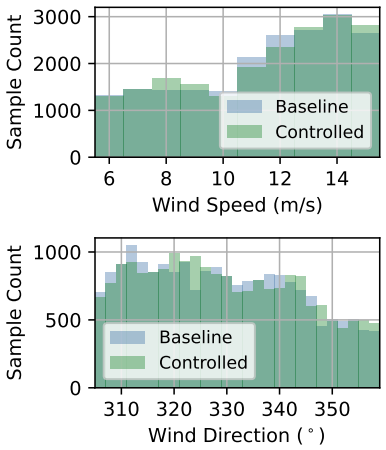

Figure 2. Number of 1-minute samples analyzed for each 1-m/s wind speed bin and 2° wind direction bin.

2.2. Wake-steering controller

To implement wake steering, yaw offsets are applied to upstream wind turbine T2 by modifying the input to the turbine's yaw controller [4, 5]. First, the wind speed (measured using the turbine's nacelle anemometer) and absolute wind direction (calculated as the sum of the nacelle position and the relative wind direction from the nacelle wind vane) are low-pass filtered to estimate the slowly varying wind conditions. The filtered signals are then used to determine the target yaw offset, which is updated at a rate of 1 Hz, via a lookup table. Finally, a modified wind vane signal, formed by subtracting the target yaw offset from the original wind vane signal, is input to the turbine's yaw controller, thereby inducing the desired yaw misalignment.

The target yaw offsets (which will be shown in Section 4) are a simplified form of the optimal offsets for maximizing the power of turbines T2 and T3 for wind speeds below 9.5 m/s, calculated using FLORIS [12]. For wind speeds above 9.5 m/s, the maximum yaw offset is gradually reduced from 20° to zero at 14.5 m/s to maintain acceptable structural loads [14]. Note that only positive yaw offsets (defined as a counterclockwise rotation of the nacelle relative to the wind direction, which deflects the wake in the clockwise direction [see Figure 1]) are used in this experiment to address the increase in blade loads observed for negative yaw misalignment [14]. Further details about the wake-steering controller are presented by Fleming *et al.* [4, 5] and Simley *et al.* [15].

3. Atmospheric conditions

We investigate the impact of atmospheric conditions on wake steering by binning the experimental data according to the following six atmospheric variables, computed in 10-minute intervals. Unless otherwise indicated, measurements are obtained from sensors on the met tower.

- Monin-Obukhov stability parameter, z/L. The Obukhov length, L, is calculated using 20-Hz measurements from a sonic anemometer at a representative height of $z = 10$ m along with pressure, humidity, and temperature sensors at heights of 5 m, 2 m, and 2 m, respectively:

$$L = -\frac{u_\star^3 T_v}{kg\overline{w'T_s'}}, \tag{1}$$

  where $u_\star$ is the friction velocity, T_v is virtual temperature, k is the von Kármán constant, g is gravitational acceleration, and $\overline{w'T_s'}$ is the kinematic heat flux. Positive and negative

values of z/L correspond to stable and unstable ABLs, respectively.

- Turbulence intensity (TI). Turbulence intensity is given by the standard deviation of the de-trended wind speed time series (with the line of best fit subtracted) measured by a cup anemometer at a height of 60 m, normalized by the mean wind speed, over a 10-minute period using 1-second data.
- Turbulent kinetic energy (TKE). Turbulent kinetic energy is calculated using de-trended wind speed component time series measured over a 10-minute period by a sonic anemometer at a 50-m height with a sampling frequency of 20 Hz:

$$\mathrm{TKE} = 0.5\sqrt{u'^2 + v'^2 + w'^2}, \tag{2}$$

where u', v', w' are the fluctuations of the streamwise, spanwise, and vertical components of wind speed, respectively.

- Wind shear exponent, α. The power-law wind shear exponent is calculated using 10-minute average wind speeds measured by sonic anemometers at heights of 10 m and 50 m.
- Integral length scale, ℓ. The integral length scale, which characterizes the largest eddy size of the turbulence, is defined as $\ell = U \cdot T_{xx}$, where U is the mean wind speed along the streamwise (mean) wind direction and the integral time scale, T_{xx}, is defined as

$$T_{xx} = \int_0^\infty u'(t)u'(t+\tau)/\sigma_{u'}^2 d\tau, \tag{3}$$

where u' is the fluctuating component of the streamwise wind speed, determined using 20-Hz sonic anemometer measurements at a height of 10 m over a 30-minute period. Equation 3 is estimated as the area under the autocorrelation function of u', truncated at the time lag, τ, where the autocorrelation decreases below 0.05.

- Wind direction standard deviation, σ_{WD}. The standard deviation of the absolute wind direction is calculated using the sum of 1-second nacelle position and nacelle wind vane measurements from turbine T2 over a 10-minute period.

Conditional distributions of each atmospheric variable during the experiment, along with the 25^{th}, 50^{th}, and 75^{th} percentiles, are shown in Figure 3, grouped by 1-m/s wind speed bins. Note that the atmospheric variables are correlated with one another to varying degrees; we observed particularly strong positive correlations between z/L and α and between TI, TKE, and σ_{WD}.

4. Analysis methods

In this section, we outline the data processing steps and performance metrics used to determine the impact of atmospheric conditions on wake steering.

4.1. Initial data processing

Prior to analyzing the experimental data, the 1-second supervisory control and data acquisition data from the wind turbines are downsampled to 1-minute averages and combined with the 10-minute atmospheric variables described in Section 3; the use of 1-minute averages represents a trade-off between averaging small-scale turbulent fluctuations and distinguishing between time-varying wind conditions. Next, using status variables and manual inspection, the data are filtered to ensure that only samples for which test turbines T2 and T3 as well as reference turbines T1 and T5 have been operating normally (i.e., not curtailed, derated, or shut down for other reasons) for at least 2 minutes are kept. Additionally, samples within 5 minutes of a change between the baseline and wake-steering control modes are discarded to remove yaw controller transients from the analysis. Further data processing, discussed by Simley *et al.* [7],

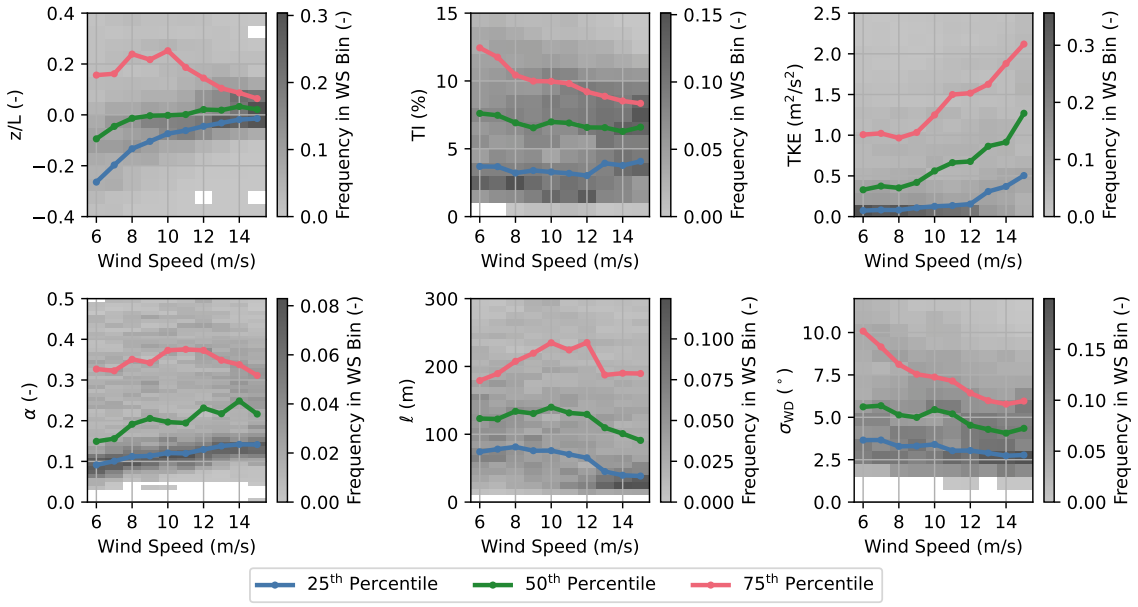

Figure 3. Frequencies of different atmospheric variables during the experiment within each 1-m/s wind speed bin along with 25$^{\text{th}}$, 50$^{\text{th}}$, and 75$^{\text{th}}$ percentiles.

is used to remove biases between the reference wind speed and power variables (measured by turbines T1 and T5) and the wind speed and power of test turbine T2. For 1-m/s wind speed bins and overlapping 5° wind direction bins, the reference variables are normalized by the ratios between the mean values of the corresponding variables at turbine T2 and the reference turbines.

As a final step prior to data analysis, the operational data are binned into 1-m/s wind speed bins and 2° wind direction bins, centered on integer wind speeds from 6 to 15 m/s and wind directions from 306° to 358°, respectively. The final data set contains 40,356 1-minute samples, or a total of roughly 28 days of data, between January 17, 2019, and January 30, 2020.

4.2. Wake-steering performance assessment

To assess the impact of atmospheric conditions on the effectiveness of wake steering, data corresponding to each 1-m/s wind speed bin are further divided into two equally sized subsets, in which the atmospheric variable of interest is either less than or greater than its median value. For both subsets, three wake-steering performance metrics are computed, as described below. The performance metrics corresponding to the two atmospheric condition bins are then compared.

First, to evaluate the ability of the wake-steering controller to achieve the intended yaw offsets in different atmospheric conditions, the mean absolute error (MAE) between the mean yaw offsets measured by turbine T2's wind vane for each wind direction bin, $\overline{\gamma}_{\text{Control}}$, and the corresponding target yaw offsets, γ_{Target}, during wake-steering control periods, is computed as

$$\text{MAE}\left(\gamma_{\text{Control}}\right) = \frac{1}{N_{\text{WD}}} \sum_{i=1}^{N_{\text{WD}}} \left| \overline{\gamma}_{\text{Control},i} - \gamma_{\text{Target},i} \right|, \tag{4}$$

where N_{WD} is the number of 2° wind direction bins. Examples of the mean yaw offsets measured at turbine T2 along with the target offsets, as a function of wind speed, are provided in Figure 4, separated by stability parameter z/L. In general, the wake-steering controller tracks the intended yaw offsets better in more stable ABLs ($z/L \geq 50^{\text{th}}$ percentile), resulting in lower values of yaw

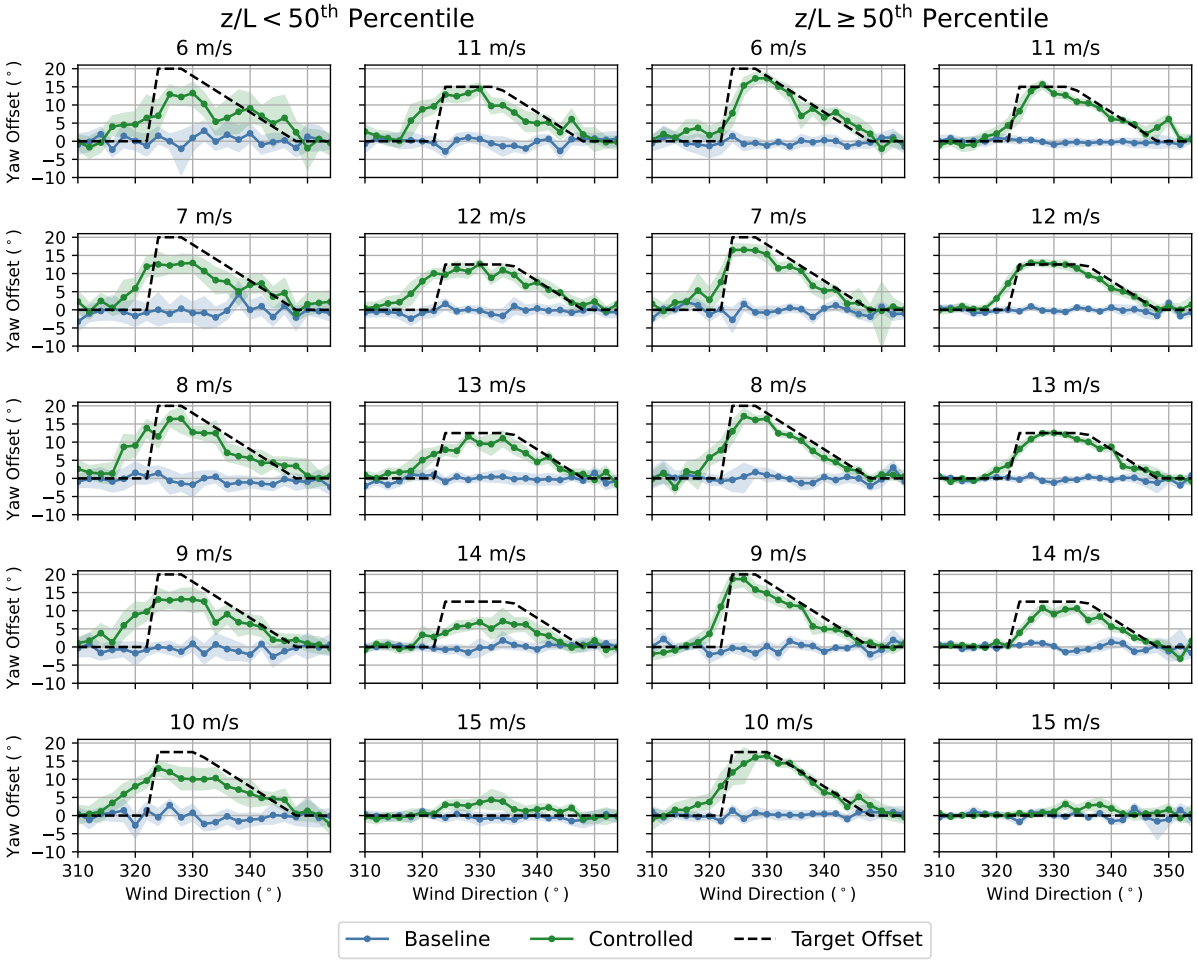

Figure 4. Mean measured and target yaw offsets as a function of wind direction for upstream wind turbine T2 during baseline and controlled periods, along with 95% confidence intervals determined through bootstrapping, for wind speed bins from 6 to 15 m/s, separated by stability.

offset MAE. As exhibited in Figure 4, wake-steering controllers tend to undershoot the intended peak yaw offsets while delivering unintended offsets outside of the wake-steering control sector, because of the inability of the controller to perfectly track variable wind directions [15, 16].

Next, to evaluate the increase in power production with wake steering for a specific wind speed bin, we examine the mean difference between the power ratio, R_{Power}, of the test and reference turbines during wake-steering and baseline control periods, over all wind direction bins:

$$\Delta\overline{R}_{\text{Power}} = \frac{1}{N_{\text{WD}}} \sum_{i=1}^{N_{\text{WD}}} \left(\frac{\overline{P}_{\text{Test,Control},i}}{\overline{P}_{\text{Ref,Control},i}} - \frac{\overline{P}_{\text{Test,Base},i}}{\overline{P}_{\text{Ref,Base},i}} \right), \tag{5}$$

where $\overline{P}_{\text{Test},i}$, and $\overline{P}_{\text{Ref},i}$ indicate the mean power produced by the test and reference turbines during baseline (Base) or wake-steering control (Control) periods for wind direction bin i. We use Equation 5 to assess the change in power for both the downstream wind turbine T3 and the mean power produced by turbines T2 and T3. Note that normalizing the mean power of the test turbines by the same quantity for the unwaked reference turbines is meant to help distinguish the impact of wake steering on power production from the influence of atmospheric conditions or

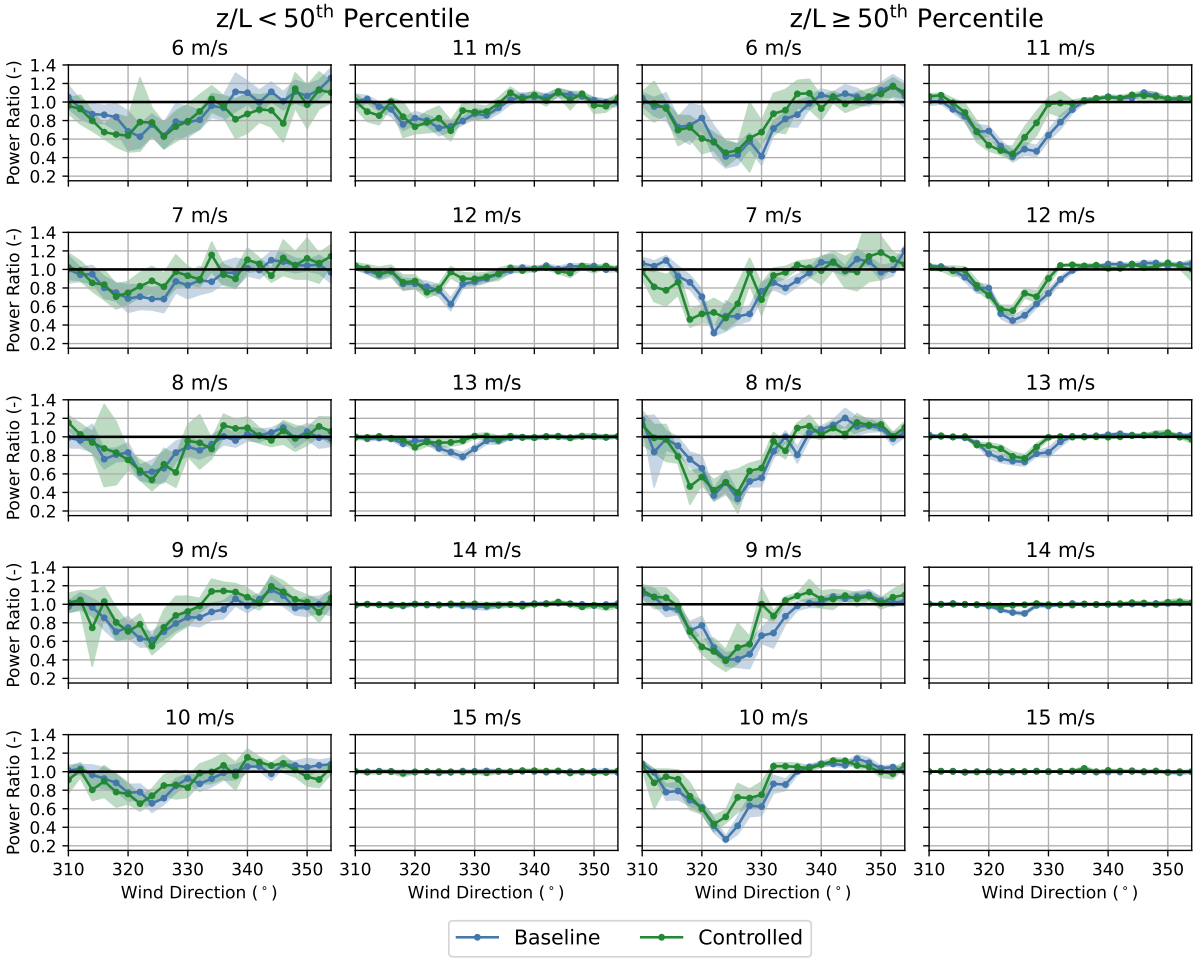

Figure 5. Power ratios for downstream wind turbine T3 during baseline and controlled periods, along with 95% confidence intervals determined through bootstrapping, for wind speed bins from 6 to 15 m/s, separated by stability.

wind turbine performance changes that are likely to affect both the test and reference turbines.

Examples of the wind direction-dependent power ratios of turbine T3 during baseline and wake-steering control periods—from which the mean change in power ratio is computed—are shown in Figure 5 for each wind speed bin, again split into two stability bins. As expected, within a given wind speed bin, the wake losses are greater during more stable ABLs [10, 11]. Note that wake losses tend to decrease as wind speed approaches rated wind speed.

Because wake losses tend to be higher in more turbulent, stable ABLs, as shown in Figure 5, it is reasonable to assume that the increase in power from wake steering is likely to be higher as well; therefore, we also compute the percentage of wake losses reduced by wake steering to provide a fairer assessment of the effectiveness of wake steering in different atmospheric conditions. Wake losses, WL, are computed as the sum of the difference between the mean power produced by the reference and test turbines, over all wind direction bins, normalized by the sum of the mean power of the reference turbines. The reduction in wake losses from wake steering is then calculated as the difference between the wake losses during baseline and wake-steering control

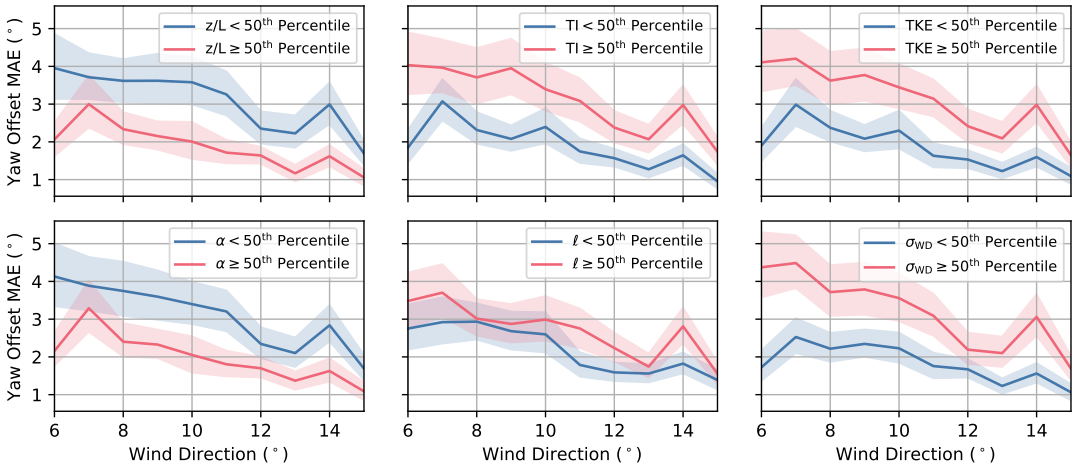

Figure 6. MAE of the wind direction-dependent mean yaw offsets of wind turbine T2 during wake-steering control periods binned by different atmospheric variables as a function of wind speed. Shaded regions indicate 95% confidence intervals.

periods relative to the baseline wake losses, which can be simplified as

$$\Delta WL = 1 - \left(1 - \frac{\sum_{i=1}^{N_{\mathrm{WD}}} \overline{P}_{\mathrm{Test,Control},i}}{\sum_{i=1}^{N_{\mathrm{WD}}} \overline{P}_{\mathrm{Ref,Control},i}}\right) \Big/ \left(1 - \frac{\sum_{i=1}^{N_{\mathrm{WD}}} \overline{P}_{\mathrm{Test,Base},i}}{\sum_{i=1}^{N_{\mathrm{WD}}} \overline{P}_{\mathrm{Ref,Base},i}}\right). \quad (6)$$

Note that Equation 6 places equal weight on all wind direction bins to improve comparability between data sets with different wind direction distributions.

Uncertainty is quantified for all three performance metrics using bootstrapping, whereby we randomly resample the underlying data sets with replacement 1,000 times to produce a distribution of values for each metric, from which 95% confidence intervals are determined. Further, to quantify uncertainty related to the choice of wind direction sector used to calculate the performance metrics (intended to encompass wind directions where nonzero mean yaw offsets occur when wake steering is active), the westernmost and northernmost wind direction bins are randomly sampled in each iteration between 306° and 314° and between 350° and 358°, respectively.

5. Results

Yaw offset MAE is plotted as a function of wind speed in Figure 6, binned according to each atmospheric variable. The computed yaw offset error is significantly lower during generally "less turbulent" conditions (i.e., periods with more stable ABLs, higher wind shear, and lower TI, TKE, and wind direction standard deviation), suggesting that the wake-steering controller tracks the intended offsets more effectively in these conditions; however, the dependence on integral length scale is relatively low. Further, yaw offset MAE decreases as wind speed increases, likely because the atmosphere tends to become less turbulent, as shown in Figure 3. We acknowledge that yaw offset MAE is an imperfect metric because the reference wind direction signal does not perfectly represent the true wind direction at turbine T2; therefore, individual yaw offset measurements may be attributed to the wrong wind direction bin, increasing the estimated yaw offset MAE. This phenomenon may affect yaw offset MAE to a greater degree in more turbulent conditions.

The mean change in power ratio and reduction in wake losses from wake steering for both downstream turbine T3 and turbines T2 and T3 combined are plotted in Figure 7 as a function

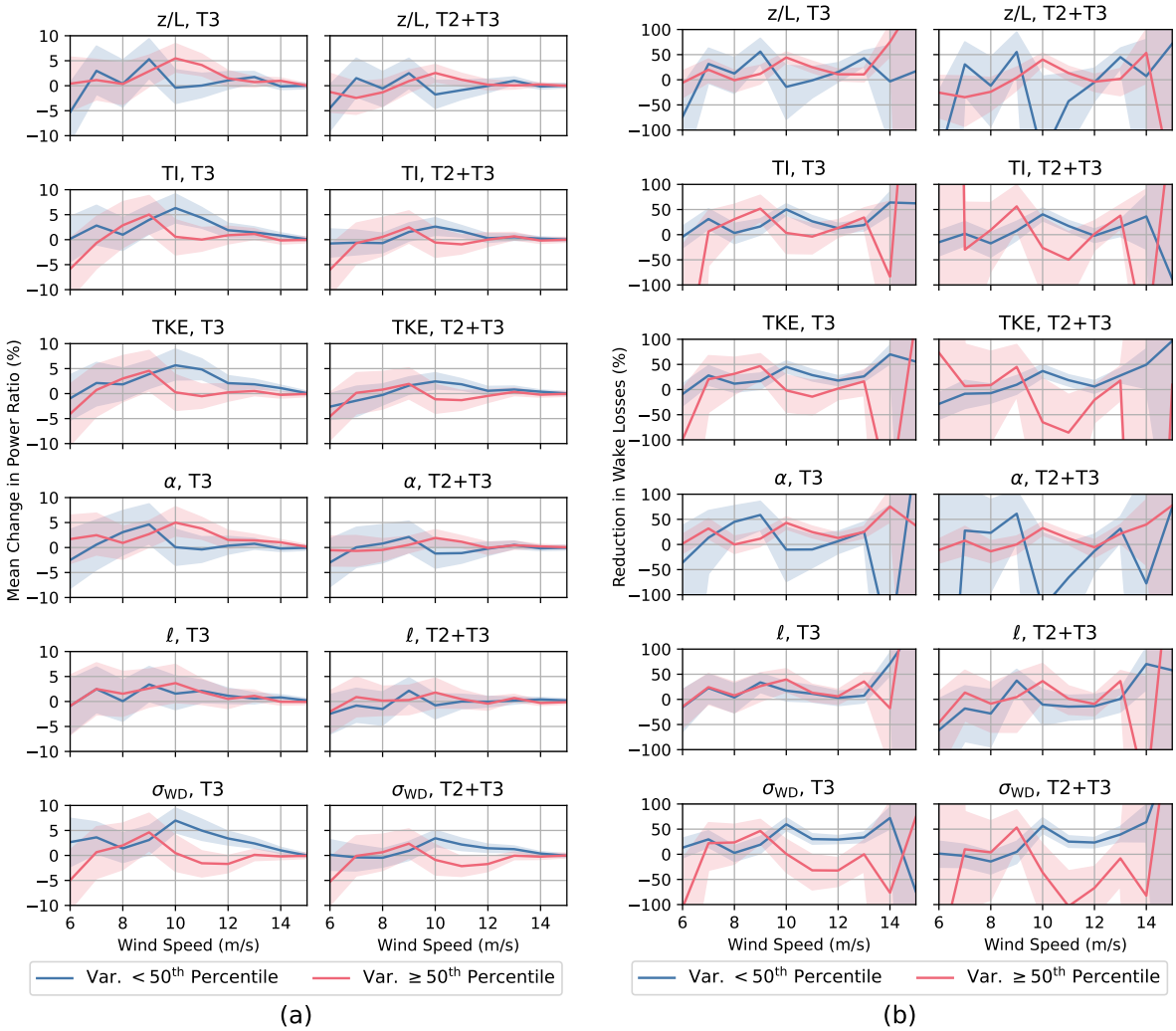

Figure 7. (a) Mean change in power ratio and (b) reduction in wake losses with wake steering binned by different atmospheric variables, as a function of wind speed, for downstream wind turbine T3 and turbines T2 and T3 combined. Shaded regions indicate 95% confidence intervals.

of wind speed, binned according to each atmospheric variable. Aside from inconclusive results for the 8-m/s and 9-m/s wind speed bins, both the power gain and the reduction in wake losses tend to be significantly higher during less turbulent conditions for turbine T3 as well as turbines T2 and T3 combined (with little dependence on integral length scale). Further, whereas wake steering tends to have a negligible or negative impact on power production during more turbulent conditions—even when only considering the power of turbine T3—it yields a net increase in power during less turbulent conditions, notwithstanding the losses at turbine T2 from yaw misalignment. Power changes very little for wind speeds above 12 m/s, primarily because of the low baseline wake losses experienced as the wind speed approaches rated wind speed (see Figure 5); low wake losses leave little opportunity for wake steering to increase power production. Additionally, the target yaw offsets for turbine T2 decrease at higher wind speeds (see Figure 4), thereby reducing the amount of wake deflection away from turbine T3.

To quantify how well wake-steering performance is characterized by the different atmospheric variables, Table 1 lists the mean differences between the performance metrics shown in Figures 6

Table 1. Mean difference between wake-steering performance metrics calculated using values of atmospheric variables less than and greater than the 50$^{\text{th}}$ percentile of the variable, over all wind speed bins (only wind speed bins between 7 and 13 m/s are used for the wake loss reduction metrics). Corresponding 95% confidence intervals are provided in brackets.

Variable	Yaw Offset MAE (°)	$\Delta\overline{R}_{\text{Power}}$ T3 (%)	$\Delta\overline{R}_{\text{Power}}$ T2+T3 (%)	ΔWL T3 (%)	ΔWL T2+T3 (%)
z/L	1.2 [1.0, 1.4]	-1.2 [-2.6, 0.2]	-0.3 [-1.3, 0.8]	3 [-12, 17]	-11 [-96, 21]
TI	-1.2 [-1.5, 0.0]	1.9 [0.5, 3.3]	0.9 [-0.0, 2.0]	3 [-9, 17]	9 [-16, 44]
TKE	-1.3 [-1.5, 0.0]	1.8 [0.4, 3.1]	0.8 [-0.3, 1.8]	11 [-4, 26]	25 [-4, 71]
α	1.1 [0.9, 1.3]	-1.4 [-2.8, -0.1]	-0.5 [-1.6, 0.5]	-3 [-19, 13]	-17 [-122, 21]
ℓ	-0.5 [-0.7, 0.0]	-0.1 [-1.7, 1.4]	-0.4 [-1.5, 0.7]	-8 [-20, 5]	-17 [-39, 3]
σ_{WD}	-1.4 [-1.6, 0.0]	3.0 [1.6, 4.4]	1.6 [0.6, 2.6]	25 [12, 41]	40 [15, 72]

and 7 for the two atmospheric condition bins, over all wind speeds. Note that differences in wake loss reduction are only averaged over wind speeds from 7 to 13 m/s because of the large uncertainty in the 6-m/s bin as well as for wind speeds above 13 m/s (see Figure 7). Out of the six variables, wind direction standard deviation is the best predictor of wake-steering performance across all metrics, considering the power of turbine T3 as well as turbines T2 and T3 combined. The next best indicators of the effectiveness of wake steering appear to be TI and TKE.

6. Conclusions

In this paper, we analyzed data from a two-turbine wake-steering experiment at a commercial wind plant to assess how well six variables describing atmospheric conditions are able to predict wake-steering performance. We found that both the power gain and wake loss reduction from wake steering, averaged over the wind directions where wake steering is active, are significantly higher during generally less turbulent atmospheric conditions (although the cause of similar wake-steering performance regardless of atmospheric conditions for wind speeds from 8 to 9 m/s requires further investigation). The wake-steering controller also appears to achieve the intended yaw offsets more effectively in these wind conditions, likely contributing to the higher power gains. Although all variables exhibit some correlation with the effectiveness of wake steering, wind direction standard deviation is the best predictor of wake-steering performance across all metrics analyzed, followed by TI and TKE. Note that the best indicators of wake-steering performance are direct measurements of the amount of variability in the wind direction or wind speed, whereas stability, wind shear, and integral length scale—which describe more general atmospheric conditions—are less effective at distinguishing performance.

Whereas the yaw offsets applied in this study were optimized for the average atmospheric conditions at the site, the strong dependence of wake-steering performance on atmospheric conditions suggests that yaw offsets should be optimized and scheduled using variables beyond wind speed and direction to maximize the effectiveness of wake steering; this would also allow for a fairer assessment of the impact of atmospheric conditions on wake steering. Further, not only is wake steering more effective during less turbulent conditions, but little or no change in power is observed for many wind speed bins the other half of the time, even for the downstream turbine alone. Consequently, it may be advantageous to only enable wake steering during particular

atmospheric conditions. Lastly, because of the relatively large uncertainty in many of the performance metrics, we did not attempt to divide the data into more than two bins for each atmospheric variable; however, when determining how to schedule yaw offsets for wake steering, the impact of atmospheric conditions should be investigated at a finer resolution.

7. Acknowledgments

This work was authored by the National Renewable Energy Laboratory, operated by Alliance for Sustainable Energy, LLC, for the U.S. Department of Energy (DOE) under Contract No. DE-AC36-08GO28308. Funding provided by the U.S. Department of Energy Office of Energy Efficiency and Renewable Energy Wind Energy Technologies Office. The views expressed in the article do not necessarily represent the views of the DOE or the U.S. Government. The U.S. Government retains and the publisher, by accepting the article for publication, acknowledges that the U.S. Government retains a nonexclusive, paid-up, irrevocable, worldwide license to publish or reproduce the published form of this work, or allow others to do so, for U.S. Government purposes.

References

[1] Boersma S, Doekemeijer B M, Gebraad P M O, Fleming P A, Annoni J, Scholbrock A K, Frederik J A and Wingerden J W V 2017 A tutorial on control-oriented modeling and control of wind farms *Proc. American Control Conf.* (Seattle, WA, USA) pp 1–18
[2] Gebraad P, Teeuwisse F, Wingerden J, Fleming P A, Ruben S, Marden J and Pao L 2016 *Wind Energy* **19** 95–114
[3] Howland M F, Lele S K and Dabiri J O 2019 *Proc. Natl. Acad. Sci. U.S.A.* **116** 14495–14500
[4] Fleming P, King J, Dykes K, Simley E, Roadman J, Scholbrock A, Murphy P, Lundquist J K, Moriarty P, Fleming K, van Dam J, Bay C, Mudafort R, Lopez H, Skopek J, Scott M, Ryan B, Guernsey C and Brake D 2019 *Wind Energy Sci.* **4** 273–285
[5] Fleming P, King J, Simley E, Roadman J, Scholbrock A, Murphy P, Lundquist J K, Moriarty P, Fleming K, van Dam J, Bay C, Mudafort R, Jager D, Skopek J, Scott M, Ryan B, Guernsey C and Brake D 2020 *Wind Energy Sci.* **5** 945–958
[6] Doekemeijer B M, Kern S, Maturu S, Kanev S, Salbert B, Schreiber J, Campagnolo F, Bottasso C L, Schuler S, Wilts F, Neumann T, Potenza G, Calabretta F, Fioretti F and van Wingerden J W 2021 *Wind Energy Sci.* **6** 159–176
[7] Simley E, Fleming P, Girard N, Alloin L, Godefroy E and Duc T 2021 *Wind Energy Sci.* **6** 1427–1453
[8] Vollmer L, Steinfeld G, Heinemann D and Kühn M 2016 *Wind Energy Sci.* **1** 129–141
[9] Hamilton N 2020 *J. Phys.: Conf. Series* **1452** 012006
[10] Barthelmie R J and Jensen L E 2010 *Wind Energy* **13** 573–586
[11] El-Asha S, Zhan L and Iungo G V 2017 *Wind Energy* **20** 1823–1839
[12] NREL 2021 FLORIS. Version 2.4.0 URL `https://github.com/NREL/floris`
[13] Bensason D, Simley E, Roberts O, Fleming P, Debnath M, King J, Bay C and Mudafort R 2021 *J. Renew. Sustain. Energy* **13** 033303
[14] Damiani R, Dana S, Annoni J, Fleming P, Roadman J, van Dam J and Dykes K 2018 *Wind Energy Sci.* **3** 173–189
[15] Simley E, Fleming P and King J 2020 *J. Phys.: Conf. Series* **1452** 012012
[16] Simley E, Fleming P and King J 2020 *Wind Energy Sci.* **5** 451–468